Hindawi Publishing Corporation
Journal of Nanomaterials
Volume 2015, Article ID 521276, 9 pages
http://dx.doi.org/10.1155/2015/521276

*Research Article*

# The Electrochemical Stability in NaCl Solution of Nanotubes and Nanochannels Elaborated on a New Ti-20Zr-5Ta-2Ag Alloy

**Claudiu Constantin Manole,[1] Cristian Pirvu,[1] Andrei Bogdan Stoian,[1] Jose M. Calderon Moreno,[2] Doina Stanciu,[3] and Ioana Demetrescu[1]**

[1]*General Chemistry Department, University Politehnica of Bucharest, Polizu 1-7, 011061 Bucharest, Romania*
[2]*Romanian Academy, Institute of Physical Chemistry "Ilie Murgulescu", Splaiul Independentei 202, 060021 Bucharest, Romania*
[3]*SC R&D Consulting and Services SRL, Strada M. Ghiculeasa 45, 023761 Bucharest, Romania*

Correspondence should be addressed to Ioana Demetrescu; ioana_demetrescu@yahoo.com

Received 9 December 2014; Revised 29 January 2015; Accepted 29 January 2015

Academic Editor: Zhenhui Kang



Nanotubular and nanochannels structures were fabricated via anodizing on a new alloy Ti-20Zr-8Ta-2Ag. A continuous coating of connected tubes/channels can be observed in the SEM micrographs forming tubular structures with diameters in hundreds of nm, as well as smaller tubes, with diameters in tens of nm. In the case of nanochannels structure, the diameters are smaller and wall thicknesses significantly thinner than in nanotubes. Wettability measurements indicate a decrease of contact angles in both cases of nanotubes and nanochannels, but the increase of hydrophilic character is more significant in the case of nanochannels. The Tafel procedure and electrochemical impedance spectroscopy tests performed in NaCl 0.9% solution indicate a better stability for the nanostructured surfaces compared to untreated alloy, the surface with nanochannels offering higher corrosion resistance. Spectral UV-VIS determination has confirmed Ag metallic presence, opening the door for applications not only in tissue engineering but for water splitting and the photoreduction of $CO_2$ as well.

## 1. Introduction

Tailoring materials into nanostructure offers a large number of opportunities in the exploitation by enhancements of their properties. In this approach, surface modification of Ti alloys has potential for wide range of applications in tissue engineering, energy, and environment. New Ti bioalloys with nontoxic elements are required for the last generation of advanced orthopedic implants, which need to satisfy more restrictive requirements regarding corrosion and stability in order to extend their service life and to reach more performance. The Al and V substitution in commercial Ti bioalloys with more safety elements and better mechanical properties reducing elasticity modulus and implying values close to human bone (30 GPa) [1, 2] involves important efforts. In this context the new alloys with Nb, Ta, and Zr [3, 4] are considered safe and nonallergenic due to their corrosion resistance and compatibility with tissue, having also high mechanical resistance. Nowadays, Ta is the most corrosion resistant and most biocompatible metal in use. Ta is not affected by chemical attack at temperatures under 150°C (ASTM B 521-12) due to its oxides surface; Ta is very ductile but has a high melting temperature (3017°C) and a very high density (16.69 g/cm$^3$); there are no reports regarding harmful effect on working people health after industrial exposure; at the contact with tissues Ta is inert. There are only few papers about Ti-Ta alloys for orthopedic applications [5–8]. Zhou and Niinomi [8] have elaborated binary Ti-Ta alloys with various amounts of Ta having high values for Young's Modulus, nonsuitable for orthopedic implants: Ti-30Ta alloy has a 70 GPa modulus, Ti-40Ta 82 GPa, and Ti-50Ta 89 GPa; only Ti-25Ta has a 64 GPa modulus and a good ratio strength/modulus, compared to other Ti-Ta alloys. Some authors [9] have elaborated on the surface of Ti-$x$Ta ($x$ = 13, 25, 50, 80%) alloys nanotubes with increased bioactivity. These alloys have shown a biphase structure influencing the nanotubes

homogeneity; the surface of Ti-80Ta was the only one where homogenous nanotubes have been formed. On the other alloys surface, the layers of nanotubes have been formed randomly, thus leading to an irregular surface. Other researchers [10] have studied the behaviour of three Ti-$x$Ta ($x = 30, 40, 50\%$) binary alloys in simulated physiological solutions (solutions 0.1 M NaCl and Ringer) finding that chemical activity is more visible in the case of alloys with higher Ta content.

Zr has demonstrated a good mechanical strength, high corrosion resistance, and biocompatibility. Zr is an isomorphic element which is soluble in both titanium ($\alpha$ and $\beta$) and tantalum [11–13]. The alloy Ti-ZrNb [14] has good mechanical properties, elasticity, and machinability. Kobayashi et al. [15] have shown that Ti-50Zr has hardness 2.5 times larger than that of Ti or Zr. Other researchers have investigated binary Ti-Zr alloys with low content Zr (from 12% to 18%) and found that such alloys have suitable properties as implants [16–18]. It is worth to mention that at tissue implant fibrous capsules formed around Ti-Zr alloys [19]. The antibacterial effect of Ti-Zr alloys nanolayers and cell growth as a function of nanoarchitectures dimensions have been the object of several investigations as well [20, 21].

Silver (density 10.54 g/cm$^3$) as a ductile and antibacterial noble metal is possible to enhance resistance to corrosion, electrochemical stability, mechanical properties, and antibacterial activity in binary alloys with Ti. Kang et al. [22] investigating three different alloys Ti-$x$Ag ($x = 1, 2, 4\%$) have observed a high antibacterial effect for the alloy Ti-4Ag for a 7-day period, a time when the alloy was biocompatible. Zhang et al. [23] determined excellent corrosion resistance, low ion release, and good biocompatibility for Ti-5Ag and Ti-20Ag alloys. Research had also been done on more complex alloy with Ta and/or Zr. Vasilescu et al. [24] had fabricated and evaluated electrodeposited nanolayers on a new Ti-15Ta-5Zr, while Li et al. have investigated biological properties of Ti-35Nb-5Zr [25]. Bioactive ceramic coating was recently investigated as well for the Ti-15Ta-5Zr alloy [26]. As it can be seen from the literature data, implants from Ti alloys with Ta, Zr, and Ag present controversial results regarding their properties. A way to avoid such a situation is elaboration of an innovator content of the alloying using small amount of Ta and Ag for keeping a low density of alloy (Ti has density 4.81 g/cm$^3$) and adding more Zr for mechanical resistance and hardness increase such as in the case of the present paper. The innovative alloying with Zr and Ag in the proper concentration has the role of keeping mechanical and anticorrosive properties in suitable limits inducing antibacterial protection via slow release of $Ag^+$ ions in surrounding tissue. In the present work, the formation and characterization of 1D nanoarchitectures on the Ti-20Zr-5Ta-2Ag alloy are subjected to the different conditions of anodizing treatment. The anodizing is recommended as a facile and cheap surface treatment and is investigated comparatively in this paper. The main aim is to find out the formation of surface nanostructures with best stability performance in NaCl solution. This stability is of significant importance for designing new strategies to enhance surface properties of materials with application in tissue engineering as well as in green chemistry.

## 2. Experimental

*2.1. Alloy Fabrication and Surface Characterization.* The alloy was obtained in as-cast state in a levitation furnace (Five Cells, CELLES MP 25HF) operating with a power of 25 kW, a magnetic field frequency of 215 kHz, and a melting temperature of about 2000°C. The alloy synthesis took place in two steps (melting and remelting) in a cold crucible, in levitation mode in inert gas (Ar) atmosphere, thus leading to a very homogeneous composition and avoiding the alloy contamination.

The alloy composition was determined with an X-ray fluorescence spectrometer (XEPOS 03); samples were cut from five different ingots and ground to a bright, smooth surface and then were exposed to X-ray flux of the spectrometer. The impurities level in the (as cast) titanium alloy complies with the limits of ASTM B367. In this situation an influence on electrochemical stability of the alloy is not expected.

The microstructure of the bare alloy and of the nanotubes and nanochannels were examined by scanning electron microscopy (SEM) in a FEI Quanta 3D FEG apparatus working at accelerating voltages between 5 and 20 kV equipped with secondary electrons (SE) and back scattering electrons (BSE) detectors and an energy dispersive X-ray (EDX) spectrometer for elemental chemical analysis.

*2.2. Nanoarchitectures Elaboration and Surface Characterization.* Two kinds of 1D nanoarchitectures as nanotubes and nanochannels, respectively [27, 28], were elaborated on the surface of Ti-20Zr-5Ta-2Ag, alloy.

For the nanochannels fabrication, the alloy samples were first grinded with SiC abrasive paper with roughness up to 1200. The samples were cleaned by ultrasonication in acetone and ethanol for 10 minutes each and then washed with deionized water. After drying, the samples were etched in an acid solution containing HF + $H_2SO_4$ + $H_2O$, rewashed with deionized water, and dried in atmosphere. The nanochannel formation was carried out by anodizing in a hot glycerol electrolyte containing 10%wt $KHPO_4$ in a two-electrode setup. As the working electrode the alloy was used and as counter electrode platinum. The anodizing was carried out at 180°C applying 50 V for 2 hours.

The self-ordered nanotubes were obtained by electrochemical oxidization of Ti-20Zr-5Ta-2Ag in glycerol solution with 4% $H_2O$ and 0.2 M $NH_4F$. The alloy substrate was grinded with SiC abrasive paper with roughness up to 1200. Subsequently the alloy sample was ultrasonicated for 5 min and dried at room temperature. For the nanotubes growth the working (oxidizing) electrode was the Ti-20Zr-5Ta-2Ag alloy. Two rods of graphite represent the counter electrode. Between the Ti-20Zr-5Ta-2Ag and the graphite electrode a 40 V voltage was applied from a MATRIX MPS-7163 power source.

The surface characterization of the nanotubes and nanochannels was performed with the same FEI Quanta 3D FEG apparatus as the one used for the untreated alloy. The contact angles were determined for all samples using CAM

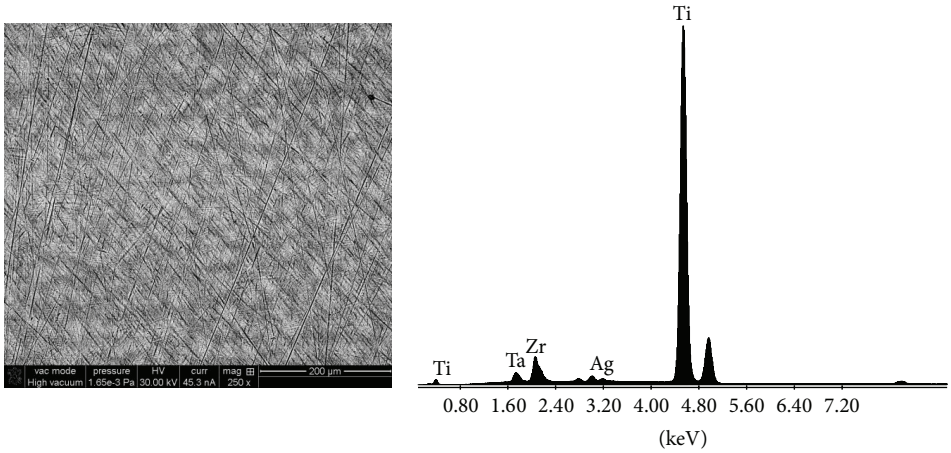


Figure 1: SEM micrograph (a) and EDX spectrum (b) for bare Ti-20Zr-5Ta-2Ag alloy.

100 equipment and software at room temperature. Each value was the average of three determinations.

*2.3. The Electrochemical Characterization.* The electrochemical characterization for nanotubes and nanochannels structures was performed with an Autolab PGStat 302N in a three-electrode configuration: a platinum counter electrode, an Ag/AgCl reference electrode, and the nanostructured Ti-20Zr-5Ta-2Ag substrate as working electrode. The electrochemical measurements and data processing were achieved with Nova 1.10 software. The testing solution for the electrochemical experiments was 0.9% NaCl saline solution and the temperature was 25°C.

*2.4. Spectral UV-VIS Determinations.* For the spectroscopic measurements, a Perkin Elmer Lambda 900 equipped with an integrating sphere module was used, and the data was recorded by means of the UV WinLab 5.2.0.0646 software.

## 3. Results and Discussion

*3.1. Surface Characterization of the New Alloy before Anodizing.* The alloy composition is as follows (%wt): 0.011% H, 0.02% N, 0.12% O, 19.968% Zr, 4.851% Ta, 1.969% Ag, 0.0581% W, 0.0071% Nb, 0.01280% Mg, 0.0492% Cd, 0.01770% Sn, 0.01057% Si, 0.0237% Cu, 0.0242% Zn, and balance Ti.

The alloy shows $\alpha + \beta$ biphase with Widmanstatten acicular microstructure (Figure 1(a)). It presents typical lamellas "colonies" of $\alpha$ and $\beta$ phases, as a result of the slight variations in the distribution of the alloying elements. Interlamellar distances are in the order of few microns. EDX spectrum (Figure 1(b)) identified the constituent elements of the alloy: Ti, Zr, Ta, and Ag; quantitative elemental analysis determined the following (wt%): 71 ± 2% Ti; 20 ± 1% Zr; 6 ± 2% Ta; 2 ± 1% Ag. According to some unpublished results (XPS), yet, the native passive film on the Ti-20Zr-5Ta-2Ag alloy surface contains the protective oxides $TiO_2$, $ZrO_2$, $Ta_2O_5$, and metallic Ag.

Regarding wettability results the average contact angle from the three measurements of the surface before anodizing is 64.54, a value which is in the hydrophilic domain.

*3.2. Surface Characterization of the 1D Nanoarchitectures on the New Alloy.* The nanostructured surface of the alloy Ti-20Zr-5Ta-2Ag is subject of Figures 2 and 3.

Hollow tubular structures with diameters in hundreds of nm can be observed in the SEM micrographs, as well as smaller tubes, with diameters in tens of nm, in the interstitial regions, forming a continuous coating of connected tubes/channels, with homogeneous walls thicknesses about 100 nm.

The elemental chemical analysis by EDX detected only the alloy elements, Ti, Zr, Ta, Ag, and O. The image taken with $Z$-contrast in BSE-SEM mode shows the distribution of Ag nanoparticles that decorates the oxide coating.

The small peak at 5 keV in the EDS corresponds to the K-beta line of titanium (Ti), which appears always accompanying the main K-alpha line at around 4.50. Only the K-alpha spectral lines have been marked on the spectra, for the sake of clarity. The sample shows the oxide coating with a structure of interconnected channels of varying diameters. The wall thickness in this sample is significantly thinner (even a few nm) than in the sample with nanotubes, with channels diameter varying from between a few tens of nm and a few hundreds of nm. Larger cavities can be observed where several channels converge.

The small bright dots in Figures 2(d) and 3(d) are silver nanoparticles on the surface of nanotubes or nanochannels.

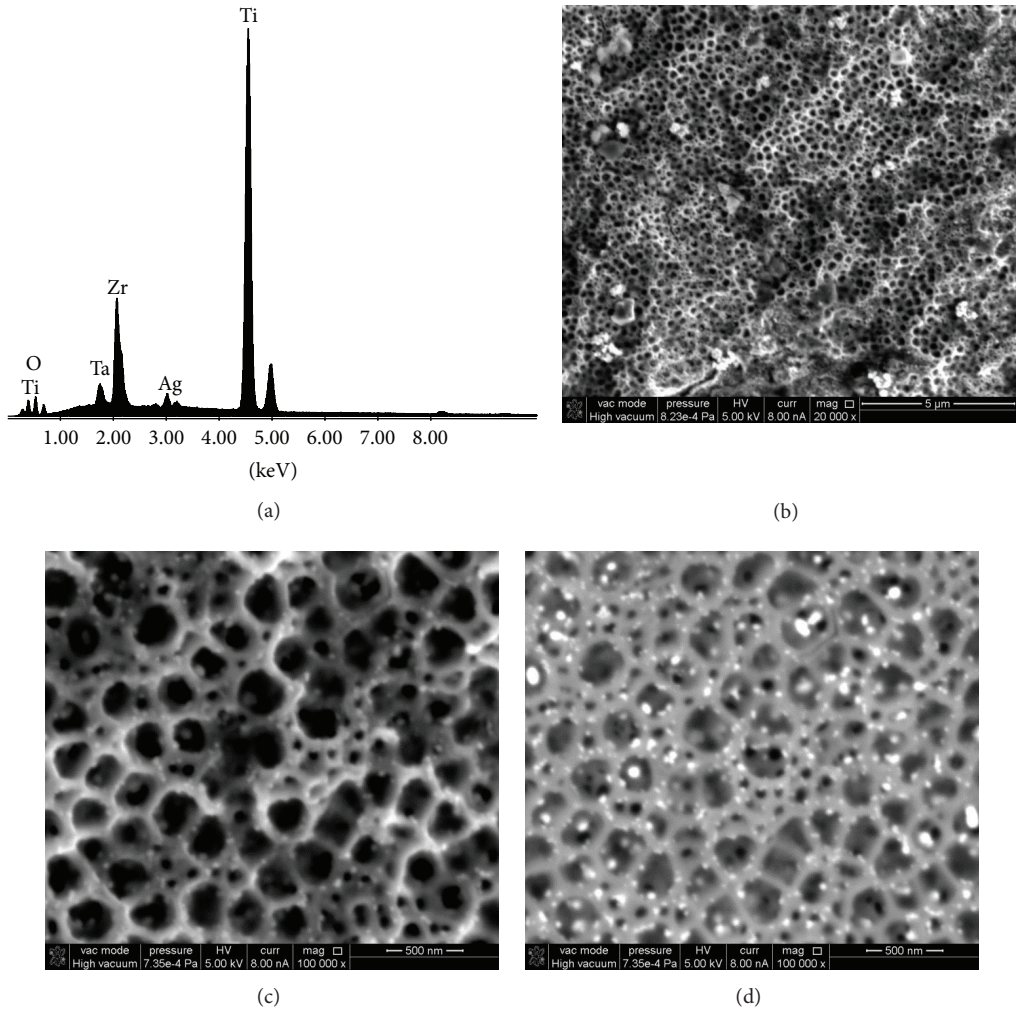


Figure 2: (a) EDX spectrum, ((b), (c)) SE-SEM micrographs at different magnification, and (d) BSE-SEM for the grown nanotubes.

Ag is an element of the alloy treated electrochemically, the tubes or channels and the Ag nanoparticles are no longer part of the alloy, and the Ag nanoparticles decorate the structures formed electrochemically by anodic oxidation of the other metallic elements of the alloy (Ti, Zr, and Ta). The remaining alloy substrate still contains Ag as alloying element.

The average contact angle values for the surface with nanotubes and nanochannels are 61.92 and 29.41, respectively, indicating an increase of hydrophilic character in both cases. The increase of hydrophilic character is more significant in the case of nanochannels.

*3.3. Electrochemical Stability of the Alloy before and after Nanoarchitectures Electrodeposition.* The Tafel plots of the bare alloy Ti-20Ta-5Zr-2Ag and of the alloy covered with nanotubes and nanochannels are presented in Figure 4.

Based on Tafel plots, electrochemical parameters as corrosion potential ($E_{corr}$), current density ($i_{corr}$), corrosion rate ($V_{corr}$), and polarization resistance have been computed and are presented in Table 1. The data establishes the class of corrosion resistance for bare alloy and for the nanostructured surfaces as well.

Table 1: Electrochemical parameters from Tafel plots.

| Ti alloy | $E_{cor}$, V | $I_{corr}$, A/cm$^2$ | $R_p$, Ω | $V_{corr}$, mm/year |
|---|---|---|---|---|
| Untreated | −0.431 | $478.5 \times 10^{-9}$ | $0.19 \times 10^{6}$ | $4.73 \times 10^{-3}$ |
| Nanochannels nanostructure | −0.010 | $12.03 \times 10^{-9}$ | $3.66 \times 10^{6}$ | $0.113 \times 10^{-3}$ |
| Nanotubes nanostructure | −0.048 | $26.24 \times 10^{-9}$ | $0.83 \times 10^{6}$ | $2.47 \times 10^{-3}$ |

As can be seen from the main corrosion parameters of Table 1, nanostructured Ti-20Ta-5Zr-2Ag alloy in NaCl solution has better value for 1D nanoarchitectures, nanotubes, and nanochannels. As expected, the resistance of nanochannels

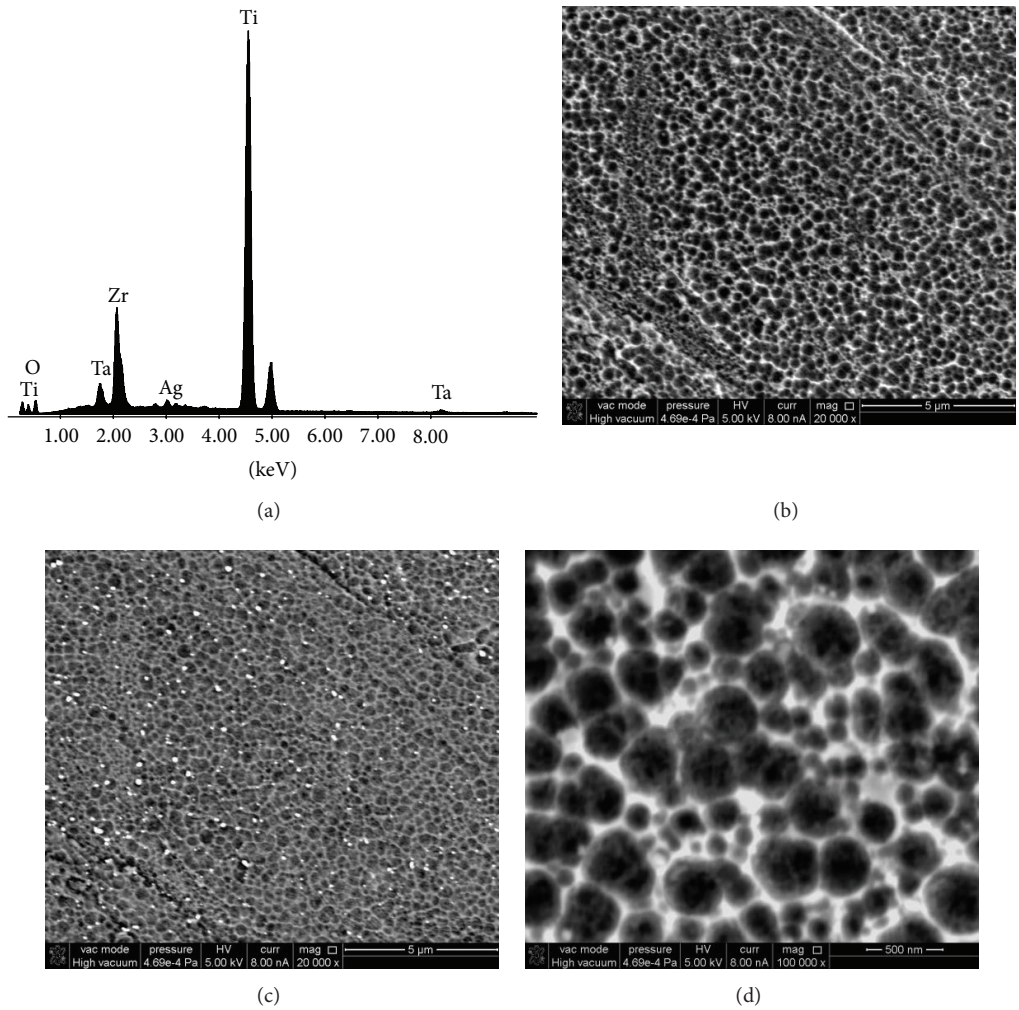


Figure 3: (a) EDX spectrum, (b) SE-SEM micrograph, and ((c), (d)) BSE-SEM micrographs at different magnifications for the grown nanochannels.

structure is bigger as an expression of the significantly thinner dimension of walls as previously observed in the SEM images of Figure 3.

According to Table 1 values the nanochannels structure has the best stability and is in the first group of corrosion resistance class, entitled "perfect stable." Both the bare alloy and the nanotubes structure are in the second group of corrosion resistance, being "very stable." The range of stability taking into account the corrosion potential as well, which is more electronegative for bare alloy, is as follows:

$$\text{Nanochannels} \longrightarrow \text{Nanotubes} \longrightarrow \text{Bare alloy}. \quad (1)$$

Electrochemical impedance spectroscopy analysis is in good correlation with Tafel analysis confirming the same hierarchy of stability. Nyquist spectra (Figure 5) recorded in NaCl solution evinced larger semicircles with bigger radii and higher impedance data for the alloys with nanostructured surface in comparison with the bare one.

For quantitative interpretation of Nyquist spectra, different equivalent circuits were proposed for untreated and coated samples, as presented in Figure 5. In the proposed circuits, $R_s$ represents the electrolyte solution resistance and parallel $R_{ox}$ and $CPE_{ox}$ elements are the resistance and constant phase element of the compact oxide layer. For treated samples the equivalent electric circuits contain a supplementary CPE parallel combination corresponding to the nanostructured oxide layers, $R_{nc}$ and $CPE_{nc}$ for nanochannels and $R_{nt}$ and $CPE_{nt}$ for nanotubes structures.

Electrical parameters of the proposed equivalent circuits obtained after fitting the results of EIS tests are presented in Table 2.

The resistance of the compact oxide layer is one order of magnitude higher for nanochannels as against untreated and nanotubes samples. The resistance of nanochannels layer is also better compared to nanotubes layer. $N$ coefficient of $CPE_{ox}$ shows an almost pure capacitive behavior for compact oxide layer of untreated sample ($N$ is 0.93) while

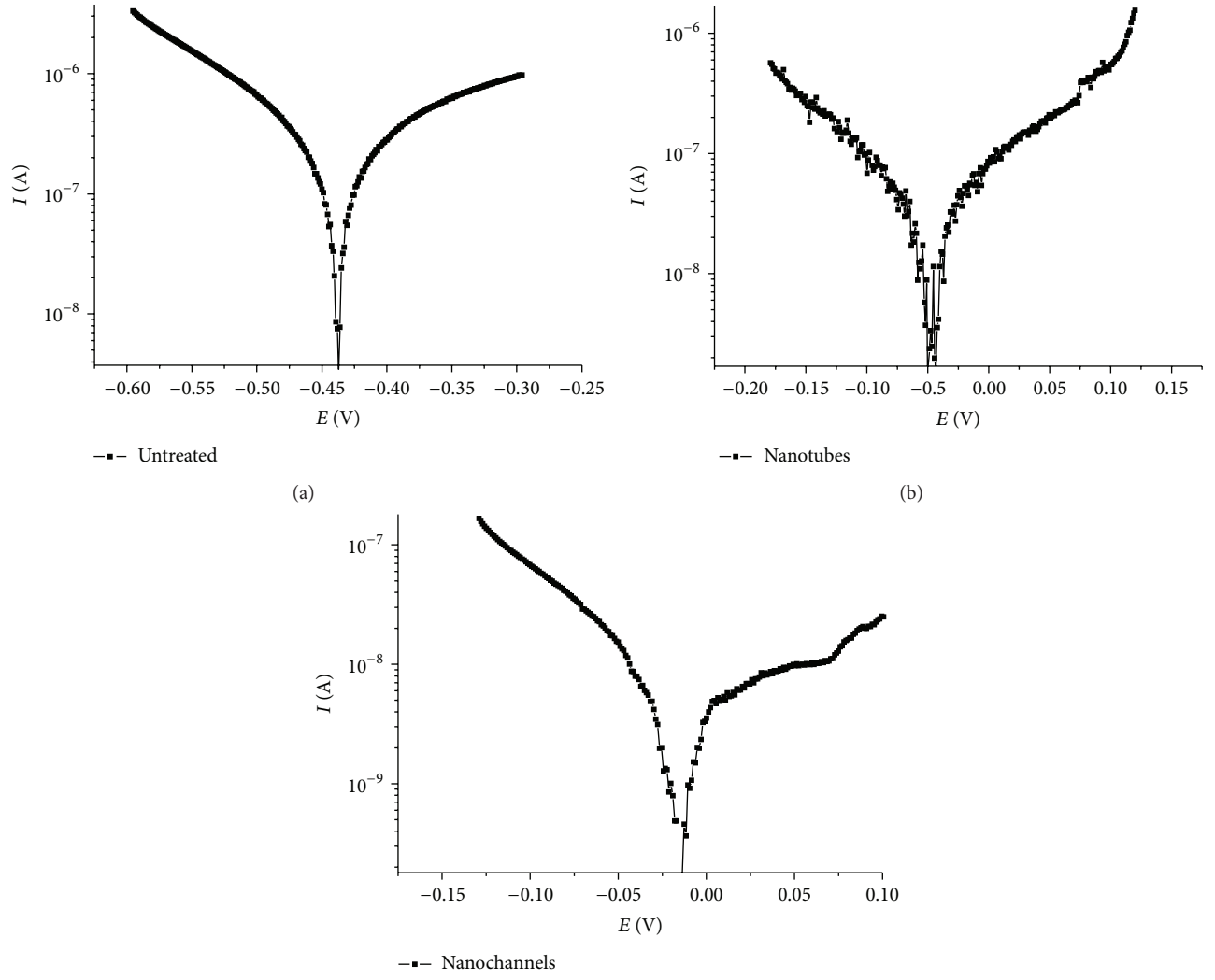


Figure 4: Tafel plots for bare and nanostructured surface of Ti-20Zr-5Ta-2Ag alloy in NaCl 0.9% for (a) untreated alloy, (b) nanotubes, and (c) nanochannels.

Table 2: EIS parameters for bare Ti-20Zr-8Ta-2Ag alloy and its modified surface with nanotubes and nanochannels.

| Structured Ti alloy type | Untreated | Nanochannels | Nanotubes |
|---|---|---|---|
| $\chi^2$ | 0.0022 | 0.0046 | 0.0053 |
| $R_s$, ($\Omega$) | 46 | 41 | 28 |
| $R_{ox}$, ($\Omega$) | $1.29 \times 10^5$ | $2.12 \times 10^6$ | $2.8 \times 10^5$ |
| $CPE_{ox}$ | | | |
| $Y0$ ($\mu$Mho) | 9.57 | 1.01 | 90.7 |
| $N$ | 0.93 | 0.72 | 0.71 |
| $R_{nc}$ ($\Omega$) | | $1.49 \times 10^5$ | |
| $CPE_{nc}$ | | | |
| $Y0$ ($\mu$Mho) | | 0.51 | |
| $N$ | | 0.74 | |
| $R_{nt}$ ($\Omega$) | | | $1.21 \times 10^5$ |
| $CPE_{nt}$ | | | |
| $Y0$ ($\mu$Mho) | | | 4.62 |
| $N$ | | | 0.89 |

for the nanostructured samples it presents a quasi-similar pseudocapacitive behavior ($N$ is 0.72 for nanochannels and 0.71 for nanotubes, resp.).

The impedance data from Table 2 confirm the fact that nanochannels surface is the most protective one. This aspect is also supported by the Tafel results.

*3.4. Spectral UV-VIS Determinations.* The metallic Ag presence is confirmed in the UV-VIS diffuse reflectance. Specific bands associated with the Ag presence can be observed in the untreated sample at around 474 nm and 516 nm (Figure 6(a)). Both bands are associated with Surface Plasmon Resonance Phenomena and their position depends on the metallic Ag shape and size [29]. The presence of the two peaks is mainly associated with the deposition matrix [29]. The highest intensity is observed for the untreated alloy. Noble Ag is also deposited on the nanotubes and nanochannels, most likely due to an electron scavenging process of $Ag^+$

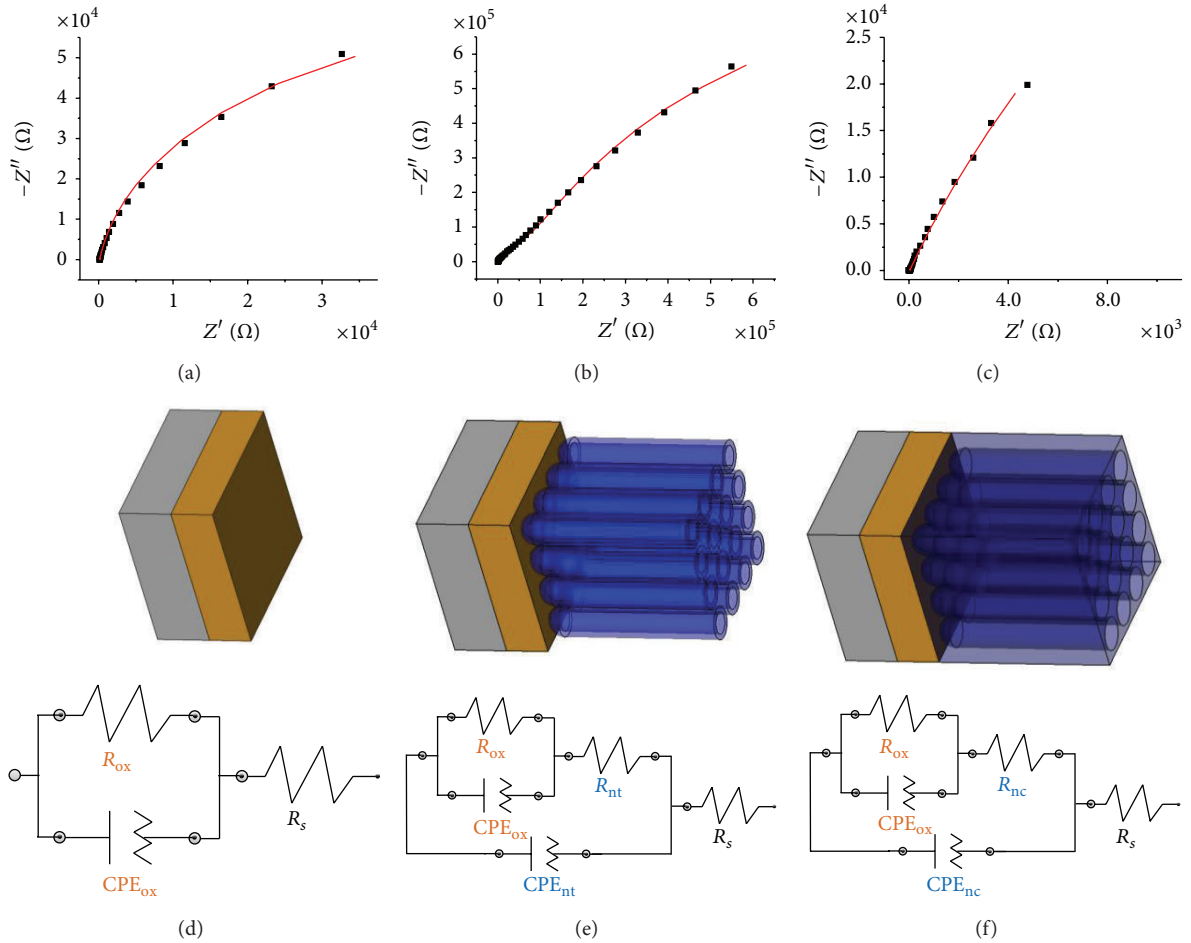


FIGURE 5: Nyquist spectra for titanium alloy (a) untreated native oxide, (b) nanochannels, and (c) nanotubes and the representation of the nanostructures with equivalent circuits for (d) native oxide, (e) nanotubes, and (f) nanochannels, used for data fitting and proposed according to the impedance spectra.

ions [30]. However, the decreased intensity indicates that for the nanostructures the presence of metallic Ag is reduced compared to the one of the bare alloy (the lowest content for the nanotubes, as highlighted in Figure 6(b)).

The nanochannels present a profile that is similar to the one of the bare substrate (Figure 6(b)). This indicates that the metallic Ag distribution is roughly similar. However, for the nanotubes (Figure 6(c)) a broad beak is observed that has a supplementary peak at 427 nm, with two shoulders at 476 nm and 507 nm. This result indicates an increased variability of the metallic Ag on the surface. The presence of metallic Ag alongside the nanostructures highlights properties of increased photocatalytic activity with possible applications for water splitting [31] and for the photoreduction of $CO_2$ and $CH_4$ [32].

## 4. Conclusions

The anodizing of a new Ti-20Zr-5Ta-2Ag alloy in specific conditions led to various types of 1D nanoarchitectures. The nanostructured surface covered with nanotubes and nanochannels has more favourable values for electrochemical parameters in NaCl 0.9% solution than those of the bare alloy. Both procedures, Tafel curves and electrochemical impedance spectroscopy, have established a range of stability with nanochannels in the first place. The surface with nanochannels is the one with the highest hydrophilic character as well. The untreated alloy has the higher contact angle indicating the lowest hydrophilic character. Based on the experimental data we can conclude that 1D nanostructures enhanced all corrosion parameters conferring superior performance to the Ti-Ta-Zr-Ag alloy and potential applications in health, energy, and environment.

## Conflict of Interests

The authors declare that there is no conflict of interests regarding the publication of this paper.

## Acknowledgments

This work was supported by Romanian UEFISCDI, Project PCE no. 242/2014. C.C. Manole expresses thanks for

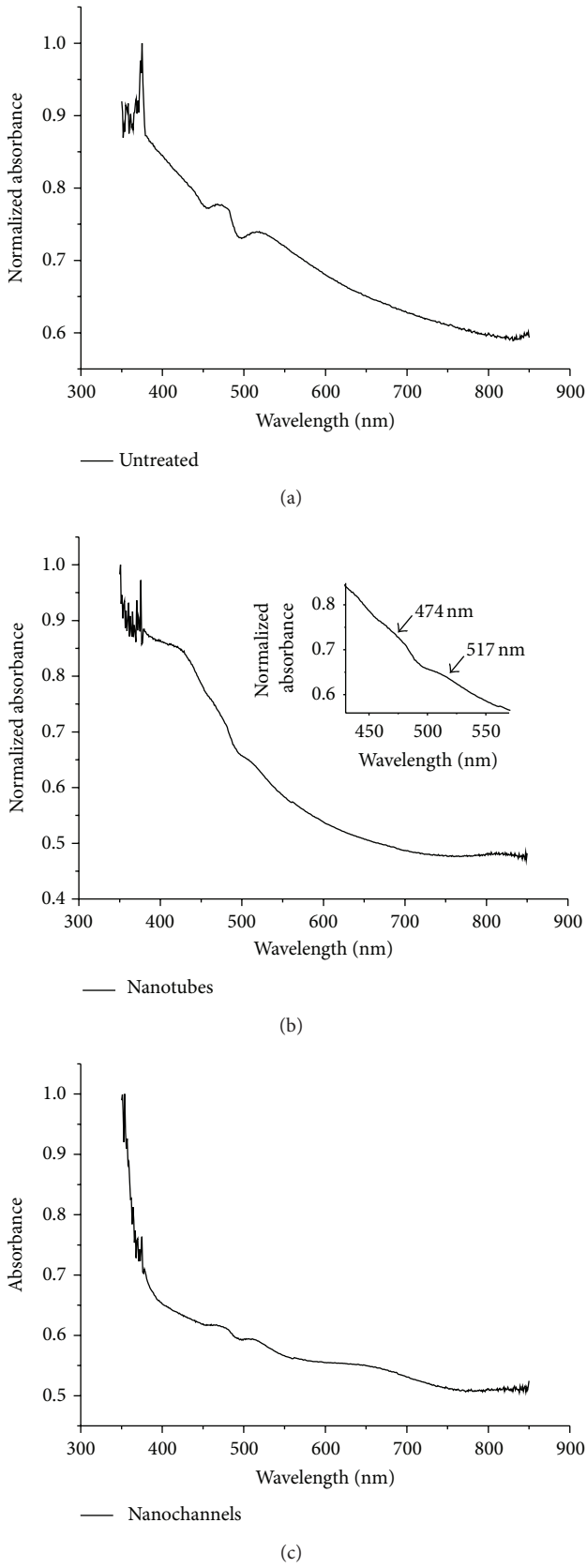


Figure 6: The UV-VIS diffuse reflectance of the (a) untreated alloy, of the (b) nanotubes with the main SPR bands highlighted in the inset, and of the (c) nanochannels.

financial support to the Sectoral Operational Programme Human Resources Development 2007–2013 of the Ministry of European Funds through the Financial Agreement POSDRU/159/1.5/S/134398.

## References

[1] P. K. Zysset, X. E. Guo, C. E. Hoffler, K. E. Moore, and S. A. Goldstein, "Mechanical properties of human trabecular bone lamellae quantified by nanoindentation," *Technology and Health Care*, vol. 6, no. 5-6, pp. 429–432, 1998.

[2] M. Staines, W. H. Robinson, and J. A. A. Hood, "Spherical indentation of tooth enamel," *Journal of Materials Science*, vol. 16, no. 9, pp. 2551–2556, 1981.

[3] E. Eisenbarth, D. Velten, M. Müller, R. Thull, and J. Breme, "Biocompatibility of $\beta$-stabilizing elements of titanium alloys," *Biomaterials*, vol. 25, no. 26, pp. 5705–5713, 2004.

[4] K. Miura, N. Yamada, S. Hanada, T.-K. Jung, and E. Itoi, "The bone tissue compatibility of a new Ti-Nb-Sn alloy with a low Young's modulus," *Acta Biomaterialia*, vol. 7, no. 5, pp. 2320–2326, 2011.

[5] Y.-L. Zhou and M. Niinomi, "Microstructures and mechanical properties of Ti-50 mass% Ta alloy for biomedical applications," *Journal of Alloys and Compounds*, vol. 466, no. 1-2, pp. 535–542, 2008.

[6] Y. L. Zhou, M. Niinomi, and T. Akahori, "Effects of Ta content on Young's modulus and tensile properties of binary Ti-Ta alloys for biomedical applications," *Materials Science and Engineering A*, vol. 371, no. 1-2, pp. 283–290, 2004.

[7] Y.-L. Zhou, M. Niinomi, and T. Akahori, "Decomposition of martensite $\alpha''$ during aging treatments and resulting mechanical properties of Ti-Ta alloys," *Materials Scence and Engineerig A*, vol. 384, no. 1-2, pp. 92–101, 2004.

[8] Y.-L. Zhou and M. Niinomi, "Ti-25Ta alloy with the best mechanical compatibility in Ti-Ta alloys for biomedical applications," *Materials Science and Engineering C*, vol. 29, no. 3, pp. 1061–1065, 2009.

[9] H. Tsuchiya, T. Akaki, J. Nakata et al., "Anodic oxide nanotube layers on Ti-Ta alloys: substrate composition, microstructure and self-organization on two-size scales," *Corrosion Science*, vol. 51, no. 7, pp. 1528–1533, 2009.

[10] G. Ciurescu, J. Izquierdo, J. J. Santana et al., "Characterization of the localized surface chemical activity of Ti-Mo and Ti-Ta alloys for biomedical applications using scanning electrochemical microscopy," *International Journal of Electrochemical Science*, vol. 7, no. 8, pp. 7404–7424, 2012.

[11] B. L. Wang, Y. F. Zheng, and L. C. Zhao, "Electrochemical corrosion behavior of biomedical Ti-22Nb and Ti-22Nb-6Zr alloys in saline medium," *Materials and Corrosion*, vol. 60, no. 10, pp. 788–794, 2009.

[12] V. Brânzoi, M. Iordoc, F. Brânzoi, G. Sbarcea, and V. Marinescu, "Surface characterization and electrochemical behavior of new biomedical Zr-based metal/ceramic composite in fetal bovine serum," *Revue Roumaine de Chimie*, vol. 55, no. 9, pp. 585–597, 2010.

[13] I. V. Branzoi, M. Iordoc, and M. Codescu, "Electrochemical studies on the stability and corrosion resistance of new zirconium-based alloys for biomedical applications," *Surface and Interface Analysis*, vol. 40, no. 3-4, pp. 167–173, 2008.

[14] W.-F. Ho, W.-K. Chen, S.-C. Wu, and H.-C. Hsu, "Structure, mechanical properties, and grindability of dental Ti-Zr alloys," *Journal of Materials Science: Materials in Medicine*, vol. 19, no. 10, pp. 3179–3186, 2008.

[15] E. Kobayashi, S. Matsumoto, H. Doi, T. Yoneyama, and H. Hamanaka, "Mechanical properties of the binary titanium-zirconium alloys and their potential for biomedical materials," *Journal of Biomedical Materials Research*, vol. 29, no. 8, pp. 943–950, 1995.

[16] Y. M. Zhang, F. Chai, J.-C. Hornez et al., "The corrosion and biological behaviour of titanium alloys in the presence of human lymphoid cells and MC3T3-E1 osteoblasts," *Biomedical Materials*, vol. 4, no. 1, Article ID 015004, 2009.

[17] J. Gottlow, M. Dard, F. Kjellson, M. Obrecht, and L. Sennerby, "Evaluation of a new titanium-zirconium dental implant: a biomechanical and histological comparative study in the mini pig," *Clinical Implant Dentistry and Related Research*, vol. 14, no. 4, pp. 538–545, 2012.

[18] B. Al-Nawas, U. Brägger, H. J. A. Meijer et al., "A double-blind randomized controlled trial(RCT) of titanium-13zirconium versus titanium grade IV small-diameter bone level implants in edentulous mandibles—results from a 1-year observation pariod," *Clinical Implant Dentistry and Related Research*, vol. 14, no. 6, pp. 896–904, 2012.

[19] Y. Ikarashi, K. Toyoda, E. Kobayashi et al., "Improved biocompatibility of titanium-zirconium (Ti-Zr) alloy: tissue reaction and sensitization to Ti-Zr alloy compared with pure Ti and Zr in rat implantation study," *Materials Transactions*, vol. 46, no. 10, pp. 2260–2267, 2005.

[20] S. Grigorescu, C. Ungureanu, R. Kirchgeorg, P. Schmuki, and I. Demetrescu, "Various sized nanotubes on TiZr for antibacterial surfaces," *Applied Surface Science*, vol. 270, no. 6, pp. 190–196, 2013.

[21] S. Grigorescu, V. Pruna, I. Titorencu et al., "The two steps nanotube formation on TiZr as scaffolds for cell growth," *Bioelectrochemistry*, vol. 98, no. 8, pp. 39–45, 2014.

[22] M.-K. Kang, S.-K. Moon, J.-S. Kwon, K.-M. Kim, and K.-N. Kim, "Antibacterial effect of sand blasted, large-grit, acid-etched treated TI-Ag alloys," *Materials Research Bulletin*, vol. 47, no. 10, pp. 2952–2955, 2012.

[23] B. B. Zhang, K. J. Qiu, B. L. Wang, L. Li, and Y. F. Zheng, "Surface characterization and cell response of binary Ti-Ag alloys with CP Ti as material control," *Journal of Materials Science and Technology*, vol. 28, no. 9, pp. 779–784, 2012.

[24] C. Vasilescu, S. I. Drob, P. Osiceanu et al., "The morphostructural, compositional, and electrochemical characterization of electrodeposited nanolayers on a new Ti-15Ta-5Zr alloy," *Journal of Nanomaterials*, vol. 2014, Article ID 369034, 12 pages, 2014.

[25] Z. Li, C. Ning, D. Ding, H. Liu, and L. Huang, "Biological properties of Ti-Nb-Zr-O nanostructures grown on Ti35Nb5Zr alloy," *Journal of Nanomaterials*, vol. 2012, Article ID 834042, 7 pages, 2012.

[26] C. Vasilescu, M. Popa, S. I. Drob, P. Osiceanu, M. Anastasescu, and J. M. Calderon Moreno, "Deposition and characterization of bioactive ceramic hydroxyapatite coating on surface of Ti-15Zr-5Nb alloy," *Ceramics International*, vol. 40, no. 9, part B, pp. 14973–14982, 2014.

[27] K. Lee, A. Mazare, and P. Schmuki, "One-dimensional titanium dioxide nanomaterials: nanotubes," *Chemical Reviews*, vol. 114, no. 19, pp. 9385–9454, 2014.

[28] D. Kowalski, D. Kim, and P. Schmuki, "$TiO_2$ nanotubes, nanochannels and mesosponge: self-organized formation and applications," *Nano Today*, vol. 8, no. 3, pp. 235–264, 2013.

[29] K.-C. Lee, S.-J. Lin, C.-H. Lin, C.-S. Tsai, and Y.-J. Lu, "Size effect of Ag nanoparticles on surface plasmon resonance," *Surface and Coatings Technology*, vol. 202, no. 22-23, pp. 5339–5342, 2008.

[30] B. Soroushian, I. Lampre, J. Belloni, and M. Mostafavi, "Radiolysis of silver ion solutions in ethylene glycol: solvated electron and radical scavenging yields," *Radiation Physics and Chemistry*, vol. 72, no. 2-3, pp. 111–118, 2005.

[31] S. C. Gomes, R. Juárez, T. Marino, R. Molinari, and H. García, "Influence of excitation wavelength (UV or visible light) on the photocatalytic activity of titania containing gold nanoparticles for the generation of hydrogen or oxygen from water," *Journal of the American Chemical Society*, vol. 133, no. 3, pp. 595–602, 2011.

[32] D. Kong, J. Z. Y. Tan, F. Yang, J. Zeng, and X. Zhang, "Electrodeposited Ag nanoparticles on $TiO_2$ nanorods for enhanced UV visible light photoreduction $CO_2$ to $CH_4$," *Applied Surface Science*, vol. 277, no. 7, pp. 105–110, 2013.